frontiers in Bioengineering and Biotechnology

ORIGINAL RESEARCH
published: 16 April 2021
doi: 10.3389/fbioe.2021.677963

Valorization of Enzymatic Hydrolysis Residues from Corncob into Lignin-Containing Cellulose Nanofibrils and Lignin Nanoparticles

Rui Xu[1,2†], Haishun Du[3†], Hui Wang[1†], Meng Zhang[1], Meiyan Wu[2], Chao Liu[2], Guang Yu[2], Xinyu Zhang[3], Chuanling Si[1], Sun-Eun Choi[4]* and Bin Li[2]**

[1] Tianjin Key Laboratory of Pulp and Paper, Tianjin University of Science and Technology, Tianjin, China, [2] Key Laboratory of Biofuels, Qingdao Institute of Bioenergy and Bioprocess Technology, Chinese Academy of Sciences, Qingdao, China, [3] Department of Chemical Engineering, Auburn University, Auburn, AL, United States, [4] Department of Forest Biomaterials Engineering, College of Forest and Environmental Sciences, Kangwon National University, Chuncheon, South Korea

OPEN ACCESS

Edited by:
Xin Zhou,
Nanjing Forestry University, China

Reviewed by:
Bo Pang,
Max Planck Institute of Colloids and Interfaces, Germany
Jing Shen,
Northeast Forestry University, China

***Correspondence:**
Chuanling Si
sichli@tust.edu.cn
Sun-Eun Choi
oregonin@kangwon.ac.kr
Bin Li
libin@qibebt.ac.cn

[†] These authors have contributed equally to this work and share first authorship

Specialty section:
This article was submitted to Industrial Biotechnology, a section of the journal Frontiers in Bioengineering and Biotechnology

Received: 08 March 2021
Accepted: 15 March 2021
Published: 16 April 2021

Citation:
Xu R, Du H, Wang H, Zhang M, Wu M, Liu C, Yu G, Zhang X, Si C, Choi S-E and Li B (2021) Valorization of Enzymatic Hydrolysis Residues from Corncob into Lignin-Containing Cellulose Nanofibrils and Lignin Nanoparticles. Front. Bioeng. Biotechnol. 9:677963. doi: 10.3389/fbioe.2021.677963

As a kind of biomass waste, enzymatic hydrolysis residues (EHRs) are conventionally burned or just discarded, resulting in environmental pollution and low economic benefits. In this study, EHRs of corncob residues (CCR) were used to produce high lignin-containing cellulose nanofibrils (LCNFs) and lignin nanoparticles (LNPs) through a facile approach. The LCNFs and LNPs with controllable chemical compositions and properties were produced by tuning the enzymolysis time of CCR and the followed homogenization. The morphology, thermal stability, chemical and crystalline structure, and dispersibility of the resultant LCNFs and LNPs were further comprehensively investigated. This work not only promotes the production of lignocellulose-based nanomaterials but also provides a promising utilization pathway for EHRs.

Keywords: lignin-containing cellulose nanofibrils, enzymatic hydrolysis residues, homogenization, corncob, lignin nanoparticles

INTRODUCTION

In recent years, along with the increasing concerns derived from fossil resource dependence and environmental pollution, lignocellulosic biomass has been regarded as an alternative source of biofuels and bio-based products because of its large amount of stock and renewability (Xu et al., 2016; Li et al., 2019, 2020; Lin et al., 2020; Yang et al., 2020; Liu K. et al., 2021; Zheng et al., 2021b). It is worth noting that agricultural residues such as wheat straw, corn stalk, bagasse, and corncob are renewable lignocellulosic biomass yet not properly managed or utilized (Anwar et al., 2019). It has been reported that approximately 900 million tons of agricultural wastes were produced in China each year (Liu et al., 2019; Xu et al., 2019; Chen et al., 2020). However, most of the agricultural wastes are often disposed by burning, which results in low economic benefits and causes severe environmental pollution. Recently, burning of agricultural waste is strictly forbidden to protect the environment and achieve the target carbon neutrality in China. Thus, it is of great importance to valorize these agricultural wastes into valuable products by using sustainable and environmentally friendly processes (Xu et al., 2020).

Recent studies suggested that converting the cellulose and hemicellulose of biomass to monomeric sugars and biofuels could be a great road to meeting the urgent need for renewable

alternative carbon resources (Robertson et al., 2017; Huang et al., 2019; Lin et al., 2019). Among the agricultural wastes, corncob has been widely concerned for its richness in hemicellulose, which is often used to produce xylose, xylitol, xylo-oligosaccharides, or furfural (Si et al., 2009b, 2013b; Zhang et al., 2014; Hu et al., 2016; Liu et al., 2016; Huang et al., 2020b). However, a large amount of corncob residue is produced and it is usually used for burning to generate heat or electricity, cultivation, feed, or just discarded. Yet, corncob residues contain abundant cellulose and lignin, which provide the possibility of creating useful materials from waste biomass, which would enable us to replace artificial and non-renewable resources with renewable resources (Kaneko et al., 2006; Si et al., 2009a, 2013a). Also, enzymatic hydrolysis of corncob residue is commonly used to produce sugar/ethanol (Xie et al., 2018b; Xu et al., 2021). However, the high production cost of enzymatic hydrolysis prevents its large-scale utilization (Lin and Lu, 2021; Liu H. Y. et al., 2021). Thus, apart from optimizing the enzymolysis process parameters, making better use of the solid residues produced after enzymatic hydrolysis could be a feasible method to reduce the total cost, based on the concept of integrated biorefinery.

As a kind of biomass waste, enzymatic hydrolysis residues (EHRs) are conventionally burned for heat and power generation, resulting in low economic benefits. Actually, the EHRs contain a significant amount of lignin, a small amount of cellulose, as well as some extractives and ash, and a trace amount of hemicellulose. As a primary starting material, the EHRs are qualified to produce lignocellulosic nanomaterials (Khan et al., 2018). Moreover, the abundant lignin existing in EHRs would play a good role in some properties such as thermal stability, antioxidation properties, hydrophobicity, and stabilization (Peng et al., 2018; An et al., 2019). By the way, in the actual industrial production, high solid enzymatic hydrolysis residue has more universal application. Thanks to the special structure of EHRs, the fiber is in a scattered and short form with a significant amount of lignin. Usually, fiber with a high content of lignin is difficult to disintegrate down to nanoscale due to the cross-linked barrier properties of lignin.

Lignocellulosic nanomaterials have received much attention at the forefront of bio-based economy in which renewable biomass is used as the raw material for the production of various consumer products (Salas et al., 2014; Song, 2019; Dai et al., 2020a). Recently, cellulose nanomaterials, mainly including cellulose nanocrystals (CNCs) and nanofibers (CNFs), have attracted rapidly growing interest from both academic and industrial researchers due to their superior physiochemical properties (Du et al., 2019; Huang et al., 2020a; Liu et al., 2020; Miao et al., 2020; Wang P. et al., 2020). However, the preparation of cellulose nanomaterials is facing several challenges such as complicated purification and pretreatment process, large amount of chemical and energy consumption, and environmental issues, which limited their large-scale applications (Xie et al., 2018a; Dai et al., 2020b; Wang H. et al., 2020). Fortunately, recent studies showed that lignin-containing cellulose nanomaterials can be obtained directly from raw materials via sustainable and low-cost approaches, and the presence of lignin endows the LCNM with many advantages such as improved thermal stability, UV-blocking performance, and water barrier property (Nair et al., 2017; Wang et al., 2018; Farooq et al., 2019; Hong et al., 2020). Especially in the last few years, lignin-containing cellulose nanofibrils (LCNFs) have been gradually arousing people's interest. The preparation of LCNFs was confirmed by various approaches from different lignocellulose biomass including unbleached thermomechanical pulp, corn husk, and tobacco stalks, among others (Bian et al., 2017; Hu et al., 2018; Wang et al., 2018; Wen et al., 2019). In addition, lignin nanoparticles (LNPs) have gained significant interest among researchers in recent years, which will play a vital role in promoting lignin valorization (Chauhan, 2020; Dong et al., 2020a). It should be noted that EHRs contain much more lignin compared to unbleached pulp and most of lignocellulosic biomass (Huang et al., 2018), and it is expected that LCNFs with high lignin content or LNPs can be produced from EHRs.

In this work, the preparation of EHRs with different enzymatic hydrolysis times (48, 72, and 108 h, respectively, for comparison) was done in accordance with the previous work of our group (Chi et al., 2019), and subsequently, high-pressure homogenization treatment of the obtained EHR samples was carried out to produce LCNFs or LNPs. The physiochemical properties of the obtained LCNFs and LNPs were further comprehensively investigated. This work will promote the development of lignocellulose-based nanomaterials and provide a promising pathway for the full utilization of agricultural wastes.

MATERIALS AND METHODS

Materials

Corncob residue (CCR) was purchased from Futaste Co., Ltd. (China), where corncob was used as raw material for the manufacture of xylose and xylitol using dilute acid hydrolysis. All the chemicals (e.g., KOH, H_2SO_4) used in this study were purchased from Sinopharm Chemical Reagent Co. Ltd. and used directly without further purification. Cellulase enzyme was obtained from Qingdao Vland Biotech Inc. The activity of cellulase was 85 FPU mL^{-1}, which was measured by the standard procedure (Ghose, 1987) and the protein content of cellulase was 80 mg-protein per mL, as determined by the standard Bradford method.

Preparation of LCNFs or LNPs

Alkaline Pretreatment of CCR

To improve the enzymatic hydrolysis efficiency of cellulose and effectively utilize the alkali lignin components, the as-received CCR was pretreated with 16 wt.% KOH at 70°C for 90 min following the procedure reported previously (Chi et al., 2019). After alkaline pretreatment, the collected solid was washed with distilled water to neutral pH and stored at 4°C.

Enzymatic Hydrolysis

Enzymatic hydrolysis of the alkaline-pretreated CCR was conducted with a high solid content (20%) under 50°C for different hydrolysis times (48, 72, and 108 h, respectively), and the enzyme dosage for saccharification was 15 FPU/g-cellulose.

Finally, the EHRs were obtained by filtration and washed to neutral pH and stored at 4°C.

High-Pressure Homogenization

The obtained EHR samples were converted to LCNFs or LNPs using a high-pressure homogenizer (GYB49-10s, China). The EHRs treated in different enzymatic hydrolysis times (named EHRs-48 h, EHRs-72 h, and EHRs-108 h, respectively) were homogenized at a concentration of 2 wt.% in deionized water for three times at 30 MPa and then five times at 60 MPa. The obtained products were noted as LCNFs-48 h, LCNFs-72 h, and LNPs-108 h, respectively.

Analytical Method for Composition

The composition of EHRs was determined following the National Renewable Energy Laboratory procedure (NREL). A dried EHR sample (0.30 g) was treated with 3 mL of 72% (w/w) H_2SO_4 at 30°C for 60 min. Then, the acid concentration was diluted to 4% (w/w) by adding deionized water, and the samples were further hydrolyzed at 121°C for 60 min. The residue (Klason lignin) was filtered with deionized water under vacuum and then dried at 105°C to constant weight. The carbohydrate content in the supernatant was quantified by high-performance liquid chromatography system (HPLC, Waters-1525, United States) analysis. The contents of cellulose and hemicellulose of EHR samples were calculated based on the amount of corresponding monomeric sugars (Sluiter et al., 2008).

Morphology Analysis

The microstructure of samples was investigated by an S-4800 field-emission scanning electron microscope (SEM, Hitachi, Japan). After homogenization, the samples of LCNFs and LNPs were freeze dried. The freeze-dried samples were sprinkled on a conductive adhesive tape mounted on a specimen stub and coated with gold by a sputter coater (E-1045, Hitachi, Tokyo, Japan) before observation.

A transmission electron microscope (TEM, Hitachi, H-7650) was also used to investigate the microstructure of samples. LCNF or LNP suspensions with a concentration of 0.03% were deposited on carbon-coated TEM grids. After the drying process, the specimen was stained with 2% uranyl acetate solution for 1.5 h. Then, the excess staining solution was removed, and the samples were dried at ambient before characterization.

Thermogravimetric (TG) Analysis

The thermal stability of the freeze-dried samples was evaluated using a TGA Q600 (TA Instruments, United States) instrument at temperatures ranging from 25 to 550°C. The experiment was carried out under a nitrogen atmosphere at a heating rate of 8°C/min (Yang et al., 2007).

Fourier Transform Infrared Spectroscopy (FTIR)

FTIR spectra of EHR samples were determined using a FTIR spectrometer (Nicolet-6700, America) with a wavenumber region of 4,000–500 cm^{-1}. Freeze-dried samples were diluted with KBr using a KBr tableting process before FTIR analysis.

X-Ray Diffraction (XRD) Analysis

XRD analysis was conducted using an ADVANCE D8 X-ray diffractometer (Bruker Co., Germany) equipped with a Ni-filtered Cu Kα radiation operated at 40 kV and 30 mA. Briefly, 0.2 g freeze-dried samples was compressed into a pellet to record patterns from 5° to 60° of diffraction with a scan rate of 4°/min. The crystallinity index (CrI) was calculated according to Segal's method (Segal et al., 1959) with the subtraction of background of glass.

Zeta Potential and Dynamic Light Scattering (DLS)

The zeta potential and DLS analyses of LCNF and LNP suspensions were detected by a microscopic electrophoresis apparatus (Nano Brook 90Plus Zeta, America) and was calculated by the electrophoretic mobility. All the samples were ultrasonically treated for 20 min before analysis, and the solid concentration was around 0.05 wt.%. The measurements were conducted in triplicate for each sample, and the average data was reported.

RESULTS AND DISCUSSION

Enzymatic Hydrolysis of CCR

As mentioned in the experiment part, the corncob after dilute acid hydrolysis and the followed alkaline treatment were used as the raw material in this study. As indicated in **Table 1**, the raw material (alkaline pretreated CCR) contains majority of cellulose with a small portion of residual xylan, lignin, and extractives, which could be a great feedstock for the preparation of glucose by enzymatic hydrolysis. **Figure 1** shows the change of lignin and glucan contents in the EHRs with different enzymatic hydrolysis times. It can be clearly seen that with the increase of enzymolysis time, the content of glucan in the EHRs decreased dramatically, while the relative proportion of lignin significantly increased. The insert photos of the collected suspensions of the nanomaterial after homogenization vividly demonstrate the color change, which correlates with the lignin content. **Table 1** gives a detailed description of the changes of each component in the EHRs. We can easily see that the cellulose and lignin account for most of the compositions of the collected EHRs for all the samples. Also, the content of xylan and extractives did not change greatly with enzymolysis time due to the strong specificity of the enzyme. Notably, the glucan content in the EHRs is only around 3.2% after enzymatic hydrolysis for 108 h. Depending on

TABLE 1 | Chemical composition of raw material and EHRs treated at different enzymatic hydrolysis times.

Samples	Extractives content (%)	Glucan content (%)	Xylan content (%)	Lignin content (%)
Raw material	5.3 ± 1.1	82.2 ± 0.9	3.4 ± 0.2	2.5 ± 0.2
EHRs-48 h	8.7 ± 0.8	38.8 ± 0.6	2.6	42.1 ± 0.6
EHRs-72 h	7.1 ± 1.0	19.3 ± 0.5	2.4 ± 0.2	63 ± 0.7
EHRs-108 h	5.9 ± 0.6	3.2 ± 0.9	2.5 ± 0.1	81.5 ± 1

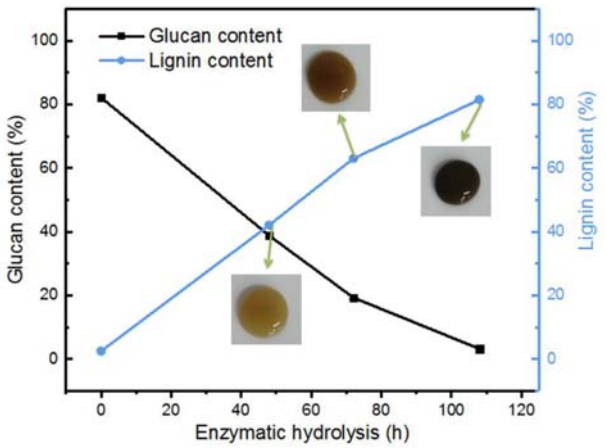

FIGURE 1 | Lignin and glucan content in the EHRs after different enzymatic hydrolysis times.

the chemical composition of the collected EHRs after enzymatic hydrolysis, we marked the samples prepared from EHRs-48 h and EHRs-72 h as LCNFs and the sample prepared from EHRs-108 as LNPs, respectively.

Morphologies of LCNFs and LNPs

Figures 2a,b show the morphology of the raw material (the alkaline-pretreated CCR) before enzymolysis. The cellulose fibers and lignin can be clearly seen, and there are some lignin particles anchored on the surface of cellulose fibers. From **Figures 2c,d**, it can be observed that the LCNFs-48 h was rich in nanofibers, and there were many irregular LNPs adhering on the nanofiber surface. **Figures 2e,f** display the morphology of LCNFs-72 h. According to these two images, the existence of nanofibers and LNPs on the surface of nanofibers could be seen clearly. **Figures 2g,h** show the morphology of LNPs-108 h, only a small number of nanofibers can be seen, and the LNPs show an obvious aggregation state (it is speculated to be the aggregate of LNPs before freeze-drying).

As shown in **Figure 3**, the morphology of LCNFs and LNPs was further examined by TEM analysis and the particle size was evaluated by DLS. From the TEM images, we can see the coexistence of nanofibers and LNPs for the samples of LCNFs-48 h and LCNFs-72 h. It should be noted that the DLS can only be used as a reference for particle distribution, not as a basis for the real particle size. As shown in **Figures 3a,b**, a large number of nanofibers with a clear fiber boundary can be seen and some of the nanofibers are anchored with some LNPs. From **Figures 3d,e**, most of the nanofibers are covered with LNPs, and the fiber boundary can be hardly observed. It can be seen from **Figures 3g,h** that LNPs with a diameter less than 50 nm can be obtained from EHRs-108 h, but it is speculated that there is still a very small amount of cellulose nanofibers embedded among them according to the component analysis results of EHRs-108 h and **Figure 3i**.

In addition, **Figure 3** indicates the measured particle size decreased with the increased lignin content in the samples. This phenomenon can be explained as follows: (1) the measured data of the sample containing nanocellulose would be larger than the actual, because of the large draw ratio. While, lignin nanoparticles can reduce the interference of draw ratio because of its near spherical shape, which lead to the measurement is closer to the actual. (2) As the lignin content increased in the samples, the possibility of attraction among the nanofibrils decreased, contributing to the separation of nanofibrils. Consequently, the measured data decreased with the increase of lignin content (Ferrer et al., 2012; Dong et al., 2020b; Pei et al., 2020; Zheng et al., 2021a).

Thermal Stability of LCNFs and LNPs

The thermal stability of the as-prepared LCNFs, LNPs, and raw materials was analyzed by TG analysis, and the results are shown in **Figure 4**. As shown in the TG and DTG curves, all samples mainly have two stages of thermal decomposition; one is before 250°C, and the other is between 250 and 400°C. For the raw material, only one weight loss peak was observed at the temperature of 350°C (T_{max}), at which the weight loss rate was around 17.5%/min. In comparison, the DTG of the LCNFs and LNPs illustrated that these samples containing the high lignin content had two weight loss peaks, and one was around 209°C and the other was around 360°C. It can also be observed from these curves that the weight loss rate at T_{max} decreased gradually along with the increase of lignin content. According to the reported literatures, the lignin decomposed slower and in a broad range (between 160 and 900°C), while cellulose decomposition usually occurred in the range of 300–400°C. The reason for the decrease of the weight loss rate at T_{max} is also related to the content of cellulose in the samples. The content of cellulose in raw material was relatively high, resulting in the high degradation rate of cellulose. However, the content of cellulose in LCNFs and LNPs decreased with the prolonging of enzymatic hydrolysis time, causing the weight loss rate decreased at T_{max}. In addition, the comparison of residual carbon produced by lignin was also consistent with the previous results (Wang et al., 2018).

Chemical and Crystalline Structures of LCNFs and LNPs

Figure 5A shows the FT-IR spectra of LCNF and LNP samples. Since no chemical reaction was performed on the lignin or cellulose during the high homogenization, all the spectra were very similar to the characteristic peak of lignin. The typical aromatic ring peaks of lignin fraction at 1,596 and 1,507 cm^{-1} were also evident (Schwanninger et al., 2004). In addition, peaks at 1,125 and 1,329 cm^{-1} were also observed, which were assigned to the condensed guaiacyl units and syringyl units of lignin, respectively (Rana et al., 2009). The peak at 1,735 cm^{-1} (C=O vibration) was observed in EHRs-48 h and EHRs-72 h, indicating the remaining of xylan in short-time EHRs (Sirvio et al., 2016). The characteristic peaks of cellulose were observed at 1,163 and 897 cm^{-1} in LCNFs-48 h and LCNFs-72 h, which was not obvious for LNPs-108 h (Schwanninger et al., 2004).

XRD patterns of the raw material and the LCNF and LNP samples are shown in **Figure 5B**. The raw material displays main characteristic diffraction peaks at 14.6°, 16.5°, 22.6°, and 34.6°, corresponding to the (1–10), (110), (200), and (004) lattice planes, respectively, indicating that the raw materials conform

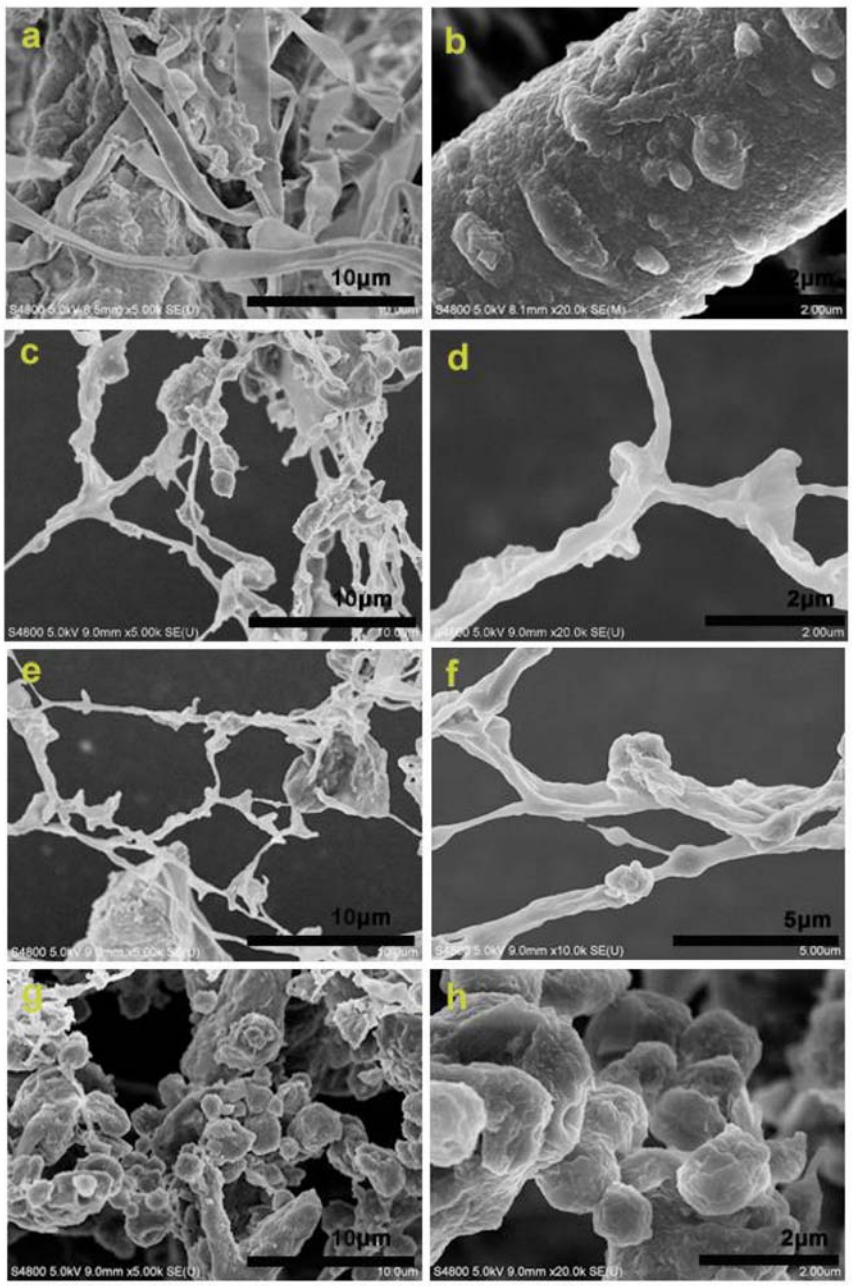

FIGURE 2 | SEM images of the raw material **(a,b)**, LCNFss-48 h **(c,d)**, LCNFs-72 h **(e,f)**, and LNPs-108 h **(g,h)**.

to the cellulose I structure (Sun et al., 2015; Du et al., 2020). On the contrary, the XRD patterns of the LCNFs and LNPs just show a broad amorphous peak, and the highest peak was around 20.5°. This could be ascribed to the removal of cellulose and the amorphous nature of lignin (Peng et al., 2018).

Dispersion Stability

The dispersion stability of LCNF and LNP suspension was evaluated by the zeta potential. It is well documented that the closer the value measured by the zeta potential was to zero, the easier the dispersion was to agglomerate and settle, and the worse the relative stability is (Herrera et al., 2018). As shown in **Figure 6A**, the zeta-potential value of the dispersion formed by LNPs-108 h was around −52 mV, indicating the best stability. It has been demonstrated that the stability of the solution would increase with the increase of lignin content, for it would improve the fibrillation process (Lahtinen et al., 2014), which increases the surface charge of the material, resulting in repulsion between the fibrils thus allowing an easier separation from each other (Rojo et al., 2015). Moreover, as shown in **Figure 6B**, all the samples

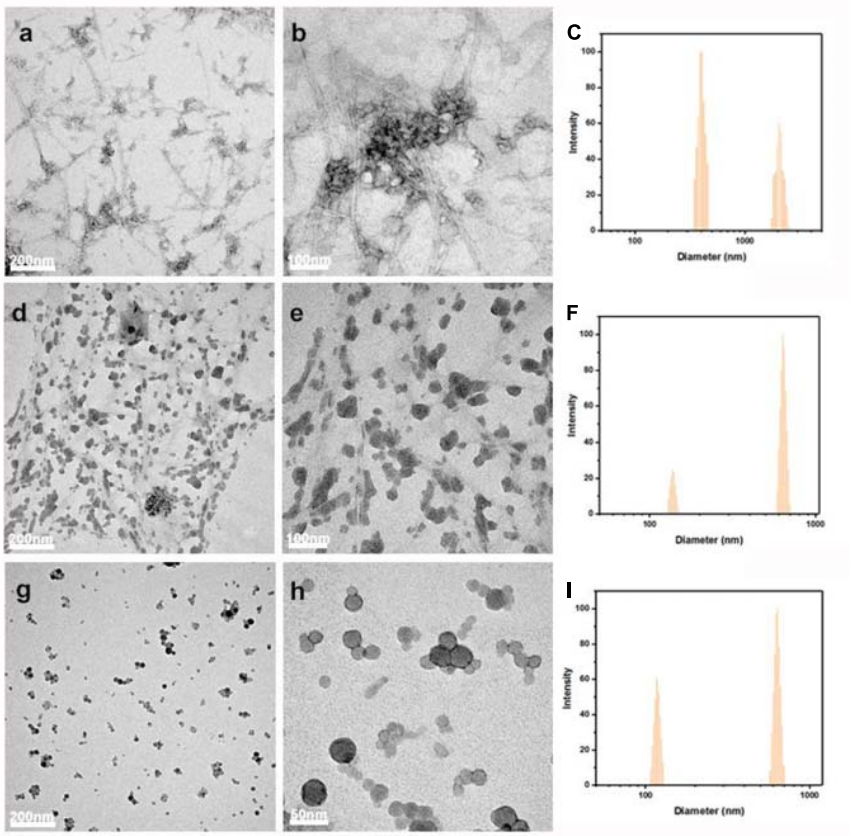

FIGURE 3 | TEM images and the measured size distribution by DLS of LCNFs-48 h **(a–c)**; LCNFs-72 h **(d–f)**; and LNPs-108 h **(g–i)**.

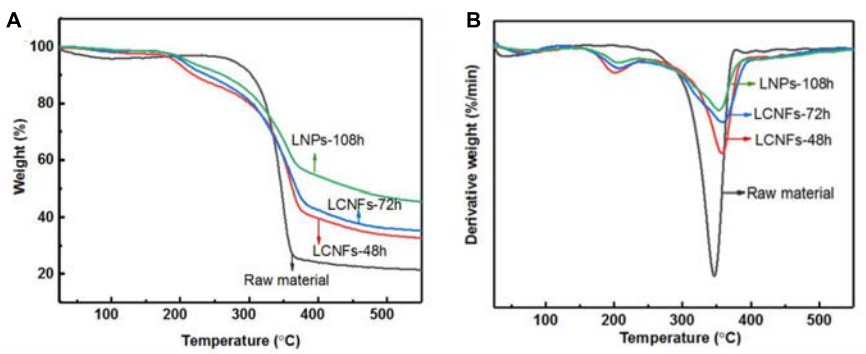

FIGURE 4 | TG **(A)** and DTG **(B)** curves of LCNFs-48 h, LCNFs-72 h, LNPs-108 h, and raw material.

exhibit very stable colloidal suspensions in aqueous media for over 1 month, indicating excellent dispersibility.

PROPOSED PROCESS FOR THE FULL UTILIZATION OF CORNCOB

Herein, based on the results obtained in this work and our previous work, we propose the full component utilization of corncob to provide a reference for the full utilization of other similar agricultural wastes. Generally, hemicellulose is extracted firstly from corncob in the industry, which mainly involves acid treatment. On the basis of the research that we had finished (Xie et al., 2018b; Chi et al., 2019), alkali treatment was a convenient way to effectively separate alkali lignin from agricultural lignocellulosic waste and promote the downstream enzymatic hydrolysis for the production of fermentable sugars. The current study demonstrated that the EHRs could be an

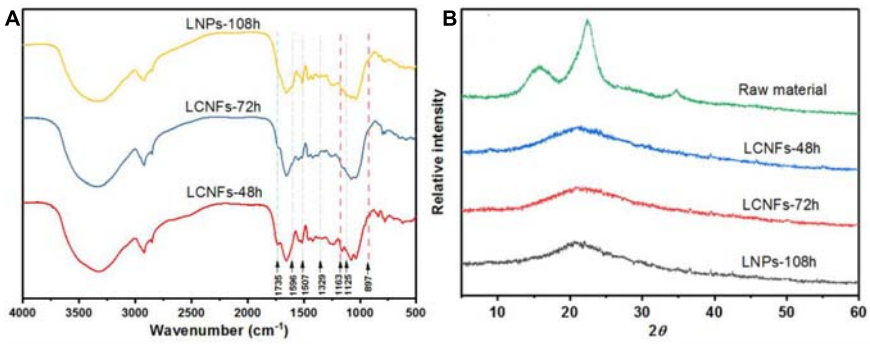

FIGURE 5 | (A) FTIR spectra of the LCNFs-48 h, LCNFs-72 h, and LNPs-108 h. **(B)** X-ray diffraction patterns of raw material and the LCNFs and LNPs samples.

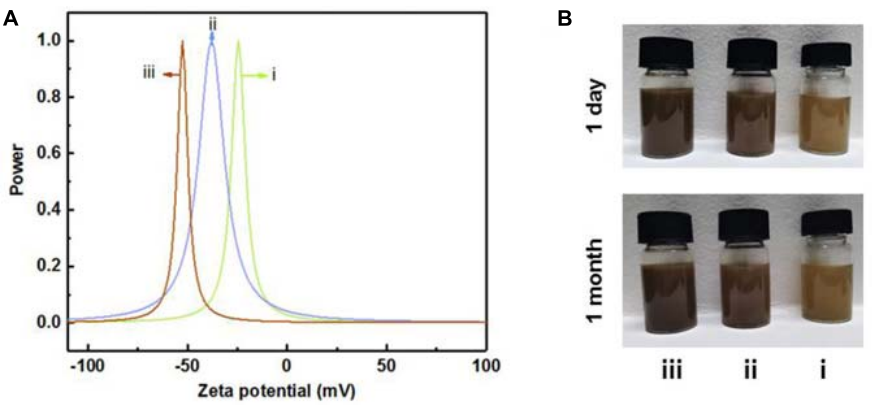

FIGURE 6 | The zeta potential **(A)** and corresponding dispersibility in water **(B)** of LCNFs-48 h (i), LCNFs-72 h (ii), and LNPs-108 h (iii).

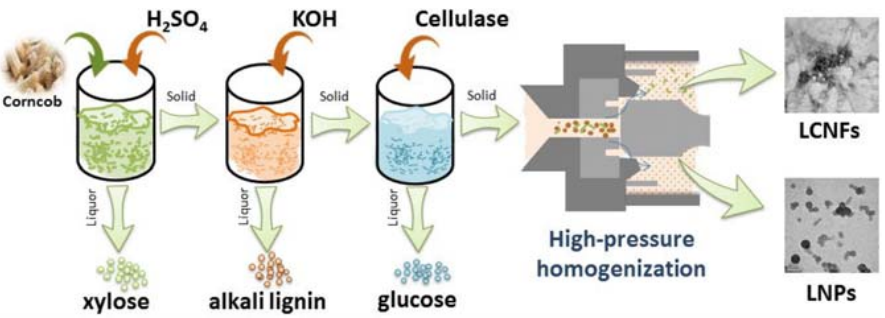

FIGURE 7 | Proposed process for the full utilization of corncob.

attractive material for the preparation of LCNFs or LNPs, which might find applications in diverse fields such as reinforcing nanofillers and Pickering emulsions. In order to show the operation involved in the proposed process more intuitively, **Figure 7** is proposed to facilitate understanding. As shown in the proposed flowchart, the solid residue produced in the previous part is used to produce the desired substance in the next step. Specifically, xylose (originated from hemicellulose) was obtained by acid treatment, alkali lignin was obtained by alkali treatment, monosaccharide (derived from cellulose) was obtained by enzymatic hydrolysis, and LCNFs with different lignin contents or LNPs could be obtained by homogenization. Thus, the comprehensive utilization of the whole components of corncob can be realized.

CONCLUSION

In summary, high LCNFs and LNPs were successfully prepared from EHRs of corncob residues via high-pressure homogenization. During enzymatic hydrolysis process, with

the increase of enzymolysis time, the lignin content increased and the cellulose content decreased resulting in the EHRs with controllable chemical compositions. It was found that the lignin content had a great influence on the morphology of the obtained nanoparticles after homogenization. The higher the lignin content in the EHRs, the smaller the size and the higher the absolute zeta potential of the obtained nanoparticles observed. This work not only promotes the development of lignocellulose-based nanomaterials but also provides a promising full utilization for the agricultural residue that simultaneously achieves the maximum use of the whole biomass.

DATA AVAILABILITY STATEMENT

The original contributions presented in the study are included in the article/supplementary material, further inquiries can be directed to the corresponding author/s.

AUTHOR CONTRIBUTIONS

RX, HD, HW, MZ, MW, CL, GY, and S-EC: investigation. CS, S-EC, and BL: supervision. RX and HD: writing—original draft. XZ, BL, S-EC, and CS: writing—review and editing. All authors contributed to the article and approved the submitted version.

FUNDING

This work was supported by the National Natural Science Foundation of China (No. 31870568) and Shandong Provincial Natural Science Foundation for Distinguished Young Scholar of China (No. ZR2019JQ10) to BL, and the Technology development Program (No. S3030198) funded by the Ministry of SMEs (MSS, South Korea) to S-EC. In addition, HD acknowledges the financial support from the China Scholarship Council (No. 201708120052).

REFERENCES

An, L., Si, C., Wang, G., Sui, W., and Tao, Z. (2019). Enhancing the solubility and antioxidant activity of high-molecular-weight lignin by moderate depolymerization via in situ ethanol/acid catalysis. *Ind. Crops Prod.* 128, 177–185. doi: 10.1016/j.indcrop.2018.11.009

Anwar, Z., Gulfraz, M., and Irshad, M. (2019). Agro-industrial lignocellulosic biomass a key to unlock the future bio-energy: a brief review. *J. Radiat. Res. Appl. Sci.* 7, 163–173. doi: 10.1016/j.jrras.2014.02.003

Bian, H., Chen, L., Dai, H., and Zhu, J. Y. (2017). Integrated production of lignin containing cellulose nanocrystals (LCNC) and nanofibrils (LCNF) using an easily recyclable di-carboxylic acid. *Carbohydr. Polym.* 167, 167–176. doi: 10.1016/j.carbpol.2017.03.050

Chauhan, P. S. (2020). Lignin nanoparticles: eco-friendly and versatile tool for new era. *Bioresour. Technol. Rep.* 9:100374. doi: 10.1016/j.biteb.2019.100374

Chen, S. L., Wang, G. H., Sui, W. J., Parvez, A. M., Dai, L., and Si, C. L. (2020). Novel lignin-based phenolic nanosphere supported palladium nanoparticles with highly efficient catalytic performance and good reusability. *Ind. Crops Prod.* 145:112164. doi: 10.1016/j.indcrop.2020.112164

Chi, X., Liu, C., Bi, Y.-H., Yu, G., Zhang, Y., Wang, Z., et al. (2019). A clean and effective potassium hydroxide pretreatment of corncob residue for the enhancement of enzymatic hydrolysis at high solids loading. *RSC Adv.* 9, 11558–11566. doi: 10.1039/c9ra01555h

Dai, L., Cao, Q. W., Wang, K., Han, S. J., Si, C. L., Liu, D., et al. (2020a). High efficient recovery of L-lactide with lignin-based filler by thermal degradation. *Ind. Crops Prod.* 143:111954. doi: 10.1016/j.indcrop.2019.111954

Dai, L., Ma, M. S., Xu, J. K., Si, C. L., Wang, X. H., Liu, Z., et al. (2020b). All-lignin-based hydrogel with fast pH-stimuli-responsiveness for mechanical switching and acuation. *Chem. Mater.* 32, 4324–4330. doi: 10.1021/acs.chemmater.0c01198

Dong, H., Li, M., Jin, Y., Wu, Y., Huang, C., and Yang, J. (2020a). Preparation of graphene-like porous carbons with enhanced thermal conductivities from lignin nano-particles by combining hydrothermal carbonization and pyrolysis. *Front. Energy Res.* 8:148. doi: 10.3389/fenrg.2020.00148

Dong, H., Zheng, L., Yu, P., Jiang, Q., Wu, Y., Huang, C., et al. (2020b). Characterization and application of lignin-carbohydrate complexes from lignocellulosic materials as antioxidants for scavenging in vitro and in vivo reactive oxygen species. *ACS Sustain. Chem. Eng.* 8, 256–266. doi: 10.1021/acssuschemeng.9b05290

Du, H., Liu, W., Zhang, M., Si, C., Zhang, X., and Li, B. (2019). Cellulose nanocrystals and cellulose nanofibrils based hydrogels for biomedical applications. *Carbohydr. Polym.* 209, 130–144. doi: 10.1016/j.carbpol.2019.01.020

Du, H., Parit, M., Wu, M., Che, X., Wang, Y., Zhang, M., et al. (2020). Sustainable valorization of paper mill sludge into cellulose nanofibrils and cellulose nanopaper. *J. Hazard. Mater.* 400:123106. doi: 10.1016/j.jhazmat.2020.123106

Farooq, M., Zou, T., Riviere, G., Sipponen, M. H., and Osterberg, M. (2019). Strong, ductile, and waterproof cellulose nanofibril composite films with colloidal lignin particles. *Biomacromolecules* 20, 693–704. doi: 10.1021/acs.biomac.8b01364

Ferrer, A., Quintana, E., Filpponen, I., Solala, I., Vidal, T., Rodríguez, A., et al. (2012). Effect of residual lignin and heteropolysaccharides in nanofibrillar cellulose and nanopaper from wood fibers. *Cellulose* 19, 2179–2193. doi: 10.1007/s10570-012-9788-z

Ghose, T. K. (1987). Measurement of cellulase activities. *Pure Appl. Chem.* 59, 257–268. doi: 10.1351/pac198759020257

Herrera, M., Thitiwutthisakul, K., Yang, X., Rujitanaroj, P.-o, Rojas, R., and Berglund, L. (2018). Preparation and evaluation of high-lignin content cellulose nanofibrils from eucalyptus pulp. *Cellulose* 25, 3121–3133. doi: 10.1007/s10570-018-1764-9

Hong, S., Song, Y., Yuan, Y., Lian, H., and Liimatainen, H. (2020). Production and characterization of lignin containing nanocellulose from luffa through an acidic deep eutectic solvent treatment and systematic fractionation. *Ind. Crops Prod.* 143:111913. doi: 10.1016/j.indcrop.2019.111913

Hu, L., Du, H., Liu, C., Zhang, Y., Yu, G., Zhang, X., et al. (2018). Comparative evaluation of the efficient conversion of corn husk filament and corn husk powder to valuable materials via a sustainable and clean biorefinery process. *ACS. Sustain. Chem. Eng.* 7, 1327–1336. doi: 10.1021/acssuschemeng.8b05017

Hu, W., Wang, X., Wu, L., Shen, T., Ji, L., Zhao, X., et al. (2016). Apigenin-7-O-beta-D-glucuronide inhibits LPS-induced inflammation through the inactivation of AP-1 and MAPK signaling pathways in RAW 264.7 macrophages and protects mice against endotoxin shock. *Food Funct.* 7, 1002–1013. doi: 10.1039/c5fo01212k

Huang, C., Dong, H., Zhang, Z., Bian, H., and Yong, Q. (2020a). Procuring the nano-scale lignin in prehydrolyzate as ingredient to prepare cellulose nanofibril composite film with multiple functions. *Cellulose* 27, 9355–9370. doi: 10.1007/s10570-020-03427-9

Huang, C., Lin, W., Lai, C., Li, X., Jin, Y., and Yong, Q. (2019). Coupling the post-extraction process to remove residual lignin and alter the recalcitrant structures for improving the enzymatic digestibility of acid-pretreated bamboo residues. *Bioresour. Technol.* 285:121355. doi: 10.1016/j.biortech.2019.121355

Huang, C., Ma, J., Zhang, W., Huang, G., and Yong, Q. (2018). Preparation of lignosulfonates from biorefinery lignins by sulfomethylation and their application as a water reducer for concrete. *Polymers* 10:841. doi: 10.3390/polym10080841

Huang, C., Zheng, Y., Lin, W., Shi, Y., Huang, G., and Yong, Q. (2020b). Removal of fermentation inhibitors from pre-hydrolysis liquor using polystyrene divinylbenzene resin. *Biotechnol. Biofuels* 13:188. doi: 10.1186/s13068-020-01828-3

Kaneko, T., Thi, T. H., Shi, D. J., and Akashi, M. (2006). Environmentally degradable, high-performance thermoplastics from phenolic phytomonomers. *Nat. Mater.* 5, 966–970. doi: 10.1038/nmat1778

Khan, A., Wen, Y., Huq, T., and Ni, Y. (2018). Cellulosic nanomaterials in food and nutraceutical applications: a review. *J. Agric. Food Chem.* 66, 8–19. doi: 10.1021/acs.jafc.7b04204

Lahtinen, P., Liukkonen, S., Pere, J., Sneck, A., and Kangas, H. (2014). A comparative study of fibrillated fibers from different mechanical and chemical pulps. *BioResources* 9, 2115–2127. doi: 10.15376/biores.9.2.2115-2127

Li, F. F., Xu, Z. W., Zhang, X. Y., Qin, W., Luo, B., and Xia, Y. (2020). Enhancement of properties of wood plastic composites by modifying lignin. *J. For. Eng.* 5, 45–51. doi: 10.13360/j.issn.2096-1359.201910010

Li, X., Xu, R., Yang, J., Nie, S., Liu, D., Liu, Y., et al. (2019). Production of 5-hydroxymethylfurfural and levulinic acid from lignocellulosic biomass and catalytic upgradation. *Ind. Crops Prod.* 130, 184–197. doi: 10.1016/j.indcrop.2018.12.082

Lin, C. Y., and Lu, C. (2021). Development perspectives of promising lignocellulose feedstocks for production of advanced generation biofuels: a review. *J. Renew. Sustain. Energy* 136:110445. doi: 10.1016/j.rser.2020.110445

Lin, W., Chen, D., Yong, Q., Huang, C., and Huang, S. (2019). Improving enzymatic hydrolysis of acid-pretreated bamboo residues using amphiphilic surfactant derived from dehydroabietic acid. *Bioresour. Technol.* 293:122055. doi: 10.1016/j.biortech.2019.122055

Lin, W., Xing, S., Jin, Y., Lu, X., Huang, C., and Yong, Q. (2020). Insight into understanding the performance of deep eutectic solvent pretreatment on improving enzymatic digestibility of bamboo residues. *Bioresour. Technol.* 306:123163. doi: 10.1016/j.biortech.2020.123163

Liu, C., Li, B., Du, H., Lv, D., Zhang, Y., Yu, G., et al. (2016). Properties of nanocellulose isolated from corncob residue using sulfuric acid, formic acid, oxidative and mechanical methods. *Carbohydr. Polym.* 151, 716–724. doi: 10.1016/j.carbpol.2016.06.025

Liu, H. Y., Xu, T., Liu, K., Zhang, M., Liu, W., Li, H., et al. (2021). Lignin-based electrodes for energy storage application. *Ind. Crops Prod.* 165:113425. doi: 10.1016/j.indcrop.2021.113425

Liu, K., Du, H., Zheng, T., Liu, H., Zhang, M., Zhang, R., et al. (2021). Recent advances in cellulose and its derivatives for oilfield applications. *Carbohydr. Polym.* 259:117740. doi: 10.1016/j.carbpol.2021.117740

Liu, W., Du, H., Zhang, M., Liu, K., Liu, H., Xie, H., et al. (2020). Bacterial cellulose-based composite scaffolds for biomedical applications: a review. *ACS Sustain. Chem. Eng.* 8, 7536–7562. doi: 10.1021/acssuschemeng.0c00125

Liu, W., Si, C. L., Du, H. S., Zhang, M., and Xie, H. (2019). Advance in preparation of nanocellulose based hydrogels and their biomedical applications. *J. For. Eng.* 4, 11–19. doi: 10.13360/j.issn.2096-1359.2019.05002

Miao, C., Du, H., Parit, M., Jiang, Z., Tippur, H. V., Zhang, X., et al. (2020). Superior crack initiation and growth characteristics of cellulose nanopapers. *Cellulose* 27, 3181–3195. doi: 10.1007/s10570-020-03015-x

Nair, S. S., Kuo, P.-Y., Chen, H., and Yan, N. (2017). Investigating the effect of lignin on the mechanical, thermal, and barrier properties of cellulose nanofibril reinforced epoxy composite. *Ind. Crops Prod.* 100, 208–217. doi: 10.1016/j.indcrop.2017.02.032

Pei, W., Chen, Z. S., Chan, H. Y. E., Zheng, L., Liang, C., and Huang, C. (2020). Isolation and identification of a novel anti-protein aggregation activity of lignin-carbohydrate complex from chionanthus retusus leaves. *Front. Bioeng. Biotechnol.* 8:573991. doi: 10.3389/fbioe.2020.573991

Peng, Y., Nair, S. S., Chen, H., Yan, N., and Cao, J. (2018). Effects of lignin content on mechanical and thermal properties of polypropylene composites reinforced with micro particles of spray dried cellulose nanofibrils. *ACS Sustain. Chem. Eng.* 6, 11078–11086. doi: 10.1021/acssuschemeng.8b02544

Rana, R., Langenfeld-Heyser, R., Finkeldey, R., and Polle, A. (2009). FTIR spectroscopy, chemical and histochemical characterisation of wood and lignin of five tropical timber wood species of the family of Dipterocarpaceae. *Wood Sci. Technol.* 44, 225–242. doi: 10.1007/s00226-009-0281-2

Robertson, G. P., Hamilton, S. K., Barham, B. L., Dale, B. E., Izaurralde, R. C., Jackson, R. D., et al. (2017). Cellulosic biofuel contributions to a sustainable energy future: choices and outcomes. *Science* 356:eaal2324. doi: 10.1126/science.aal2324

Rojo, E., Peresin, M. S., Sampson, W. W., Hoeger, I. C., Vartiainen, J., Laine, J., et al. (2015). Comprehensive elucidation of the effect of residual lignin on the physical, barrier, mechanical and surface properties of nanocellulose films. *Green Chem.* 17, 1853–1866. doi: 10.1039/c4gc02398f

Salas, C., Nypelö, T., Rodriguez-Abreu, C., Carrillo, C., and Rojas, O. J. (2014). Nanocellulose properties and applications in colloids and interfaces. *Curr. Opin. Colloid Interface Sci.* 19, 383–396. doi: 10.1016/j.cocis.2014.10.003

Schwanninger, M., Rodrigues, J. C., Pereira, H., and Hinterstoisser, B. (2004). Effects of short-time vibratory ball milling on the shape of FT-IR spectra of wood and cellulose. *Vib. Spectrosc.* 36, 23–40. doi: 10.1016/j.vibspec.2004.02.003

Segal, L., Conrad, C. M., Creely, J. J., and Martin, A. E. (1959). An empirical method for estimating the degree of crystallinity of native cellulose using the X-ray diffractometer. *Text. Res. J.* 29, 786–794. doi: 10.1177/004051755902901003

Si, C. L., Jiang, J.-Z., Liu, S.-C., Hu, H.-Y., Ren, X.-D., Yu, G.-J., et al. (2013a). A new lignan glycoside and phenolics from the branch wood of *Pinus banksiana* Lambert. *Holzforschung* 67, 357–363. doi: 10.1515/hf-2012-0137

Si, C. L., Kim, J.-K., Bae, Y.-S., and Li, S.-M. (2009a). Phenolic compounds in the leaves of populus ussuriensis and their antioxidant activities. *Planta Med.* 75, 1165–1167.

Si, C. L., Shen, T., Jiang, Y. Y., Wu, L., Yu, G. J., Ren, X. D., et al. (2013b). Antioxidant properties and neuroprotective effects of isocampneoside II on hydrogen peroxide-induced oxidative injury in PC12 cells. *Food Chem. Toxicol.* 59, 145–152. doi: 10.1016/j.fct.2013.05.051

Si, C. L., Wu, L., and Zhu, Z.-Y. (2009b). Phenolic glycosides from *Populus davidiana* bark. *Biochem. Syst. Ecol.* 37, 221–224. doi: 10.1016/j.bse.2009.01.007

Sirvio, J. A., Visanko, M., and Liimatainen, H. (2016). Acidic deep eutectic solvents as hydrolytic media for cellulose nanocrystal production. *Biomacromolecules* 17, 3025–3032. doi: 10.1021/acs.biomac.6b00910

Sluiter, A., Hames, B., Ruiz, R., Scarlata, C., Sluiter, J., Templeton, D., et al. (2008). Determination of structural carbohydrates and lignin in biomass. *Lab. Anal. Proc. (LAP)* 1617, 1–16.

Song, G. Y. (2019). The development of catalytic fractionation and conversions of lignocellulosic biomass under lignin-first strategy. *J. For. Eng.* 4, 1–10. doi: 10.13360/j.issn.2096-1359.2019.05001

Sun, B., Zhang, M., Hou, Q., Liu, R., Wu, T., Si, C., et al. (2015). Further characterization of cellulose nanocrystal (CNC) preparation from sulfuric acid hydrolysis of cotton fibers. *Cellulose* 23, 439–450. doi: 10.1007/s10570-015-0803-z

Wang, H., Xie, H., Du, H., Wang, X., Liu, W., Duan, Y., et al. (2020). Highly efficient preparation of functional and thermostable cellulose nanocrystals via H2SO4 intensified acetic acid hydrolysis. *Carbohydr. Polym.* 239:116233. doi: 10.1016/j.carbpol.2020.116233

Wang, P., Yin, B., Dong, H., Zhang, Y., Zhang, Y., Chen, R., et al. (2020). Coupling biocompatible au nanoclusters and cellulose nanofibrils to prepare the antibacterial nanocomposite films. *Front. Bioeng. Biotechnol.* 8:986. doi: 10.3389/fbioe.2020.00986

Wang, Q., Du, H., Zhang, F., Zhang, Y., Wu, M., Yu, G., et al. (2018). Flexible cellulose nanopaper with high wet tensile strength, high toughness and tunable ultraviolet blocking ability fabricated from tobacco stalk via a sustainable method. *J. Mater. Chem. A Mater.* 6, 13021–13030. doi: 10.1039/c8ta01986j

Wen, Y., Yuan, Z., Liu, X., Qu, J., Yang, S., Wang, A., et al. (2019). Preparation and characterization of lignin-containing cellulose nanofibril from poplar high-yield pulp via TEMPO-Mediated Oxidation and Homogenization. *ACS Sustain. Chem. Eng.* 7, 6131–6139. doi: 10.1021/acssuschemeng.8b06355

Xie, H., Du, H., Yang, X., and Si, C. (2018a). Recent strategies in preparation of cellulose nanocrystals and cellulose nanofibrils derived from raw cellulose materials. *Int. J. Polym. Sci.* 2018, 1–25. doi: 10.1155/2018/7923068

Xie, X., Feng, X., Chi, S., Zhang, Y., Yu, G., Liu, C., et al. (2018b). A sustainable and effective potassium hydroxide pretreatment of wheat straw for the production of fermentable sugars. *Bioresour. Technol. Rep.* 3, 169–176. doi: 10.1016/j.biteb.2018.07.014

Xu, H., Li, B., and Mu, X. (2016). Review of alkali-based pretreatment to enhance enzymatic saccharification for lignocellulosic biomass conversion. *Ind. Eng. Chem. Res.* 55, 8691–8705. doi: 10.1021/acs.iecr.6b01907

Xu, J., Liu, B., Wu, L., Hu, J., Hou, H., and Yang, J. (2019). A waste-minimized biorefinery scenario for the hierarchical conversion of agricultural straw into prebiotic xylooligosaccharides, fermentable sugars and lithium-sulfur batteries. *Ind. Crops Prod.* 129, 269–280. doi: 10.1016/j.indcrop.2018.12.002

Xu, J. Y., Shao, Z. Y., Li, Y., Dai, L., Wang, Z. J., and Si, C. L. (2021). A flow-through reactor for fast fractionation and production of structure-preserved lignin. *Ind. Crops Prod*. 164:113350. doi: 10.1016/j.indcrop.2021.113350

Xu, R., Si, C., Kong, F., and Li, X. (2020). Synthesis of γ-valerolactone and its application in biomass conversion. *J. For. Eng.* 5, 20–28. doi: 10.13360/j.issn.2096-1359.201904004

Yang, H., Yan, R., Chen, H., Lee, D. H., and Zheng, C. (2007). Characteristics of hemicellulose, cellulose and lignin pyrolysis. *Fuel* 86, 1781–1788. doi: 10.1016/j.fuel.2006.12.013

Yang, J., Si, C., Liu, K., Liu, H., Li, X., and Liang, M. (2020). Production of levulinic acid from lignocellulosic biomass and application. *J. For. Eng.* 5, 21–27. doi: 10.13360/j.issn.2096-1359.201905013

Zhang, Y., Mu, X., Wang, H., Li, B., and Peng, H. (2014). Combined deacetylation and PFI refining pretreatment of corn cob for the improvement of a two-stage enzymatic hydrolysis. *J. Agric. Food Chem.* 62, 4661–4667. doi: 10.1021/jf500189a

Zheng, L., Yu, P., Zhang, Y., Wang, P., Yan, W., Guo, B., et al. (2021a). Evaluating the bio-application of biomacromolecule of lignin-carbohydrate complexes (LCC) from wheat straw in bone metabolism via ROS scavenging. *Int. J. Biol. Macromol.* 176, 13–25. doi: 10.1016/j.ijbiomac.2021.01.103

Zheng, Y., Yu, Y., Lin, W., Jin, Y., Yong, Q., and Huang, C. (2021b). Enhancing the enzymatic digestibility of bamboo residues by biphasic phenoxyethanol-acid pretreatment. *Bioresour. Technol.* 325:124691. doi: 10.1016/j.biortech.2021.124691

Conflict of Interest: The authors declare that the research was conducted in the absence of any commercial or financial relationships that could be construed as a potential conflict of interest.